Circularly Polarized Fabry Perot Cavity Antennas with Peripheral Roughness in Superstrate Unit Cells

by

Sagar Jain

Under the supervision of

Dr. Shobha Sundar Ram

Indraprastha Institute of Information Technology Delhi
New Delhi– 110020

September 2019

Circularly Polarized Fabry Perot Cavity Antennas with Peripheral Roughness in Superstrate Unit Cells

A THESIS

Submitted in partial fulfillment of the requirements for

the degree of

Masters of Technology

by

Sagar Jain

Electronics and Communication Engineering

to
Indraprastha Institute of Information Technology Delhi
New Delhi– 110020
September 2019

Certificate

This is to certify that the thesis titled **"Circularly Polarized Fabry Perot Cavity Antennas with Peripheral Roughness in Superstrate Unit Cells"** submitted by Sagar Jain for the partial fulfillment of the requirements for the degree of Master of Technology in Electronics and Communication Engineering is a record of the bonafide work carried out by him under my guidance and supervision at Indraprastha Institute of Information Technology, Delhi. This work has not been submitted anywhere else for the reward of any other degree.

Dr. Shobha Sundar Ram
Indraprastha Institute of Information Technology, New Delhi

Abstract

A Fabry Perot cavity (FPC) antenna consists of a primary radiator at the base of a dielectric cavity sealed with a partially reflecting surface at the other end. Excitation from the radiator is partially reflected by the reflecting surface back into the cavity that is backed by a ground plane. Multiple reflections within the cavity enhances the gain of the antenna. These antennas have been extensively researched and developed for their reduced fabrication complexity and cost as compared to other high gain planar antennas. Recently, metasurfaces with desirable electromagnetic properties have been engineered for the partially reflecting surface of FPC antennas in order to reduce their profile dimensions. These surfaces usually consist of an array of unit cells that are skillfully designed in order to obtain high bandwidth or desired polarization. In this thesis, we have examined two unit cell designs - arc and rectangular loop with the diagonal - with an objective of achieving circular polarization, broad bandwidth and high gain. Based on simulations, we achieved minimum axial ratios of 7.46 dB and 7.61 dB respectively for these two designs. Then we introduced a new design parameter in the form of peripheral roughness in the edges of each of the unit cells. While the roughness did not significantly improve the axial ratio of the design with the unit cell arc, we demonstrated a wide return loss bandwidth of 202.78 MHz (8.86%), an enhanced gain of 9.48 dBi, and a reduced axial ratio of 4.79 dB for the unit cell with a rectangular loop with diagonal.

Keywords- Fabry Perot cavity antenna, superstrate, roughness.

Acknowledgment

First of all, I would like to thank my supervisor, Dr.Shobha Sundar Ram for her steadfast support and understanding throughout the entire course of my thesis. Her unwavering faith and constant encouragement have always been beneficial. Without this, this thesis would not have been completed.

I sincerely thank my parents, who always motivated me and stood by me even during my tough times. I dedicate this thesis to my parents. I am grateful to Shelly madam for her guidance in organizing the thesis contents. I would also like to thank Neeraj, Shalin, and Dinesh sir for their technical guidance.

Last but not least, I would also like to thank my lab colleagues and batchmates who directly or indirectly helped in this thesis.

Sagar Jain
MT17115
IIIT Delhi

Contents

List of Figures

List of Tables

Chapter 1

Introduction

The commonly used patch antenna is a low profile antenna that is easy to design and fabricate. However, the antenna is characterized by low gain and bandwidth [1]. One way to increase the gain is to use multiple patch elements configured as an antenna array with a single feed supporting a feed distribution network such as corporate feed network or a series feed network. However, the major disadvantage is the increase in the aperture size of the antenna and the poor efficiency of the large and complicated feed networks. Fabry Perot cavity (FPC) antennas have been explored over the last decade for their high gain and small aperture size. They are essentially single feed antennas without a complicated feed distribution network [2]. Due to their low hardware complexity and cost when compared with horn antennas and feed arrays, the FPC antenna is widely deployed in radar and communication systems.

1.1 Theory of Fabry Perot Cavity Antenna

FPC antenna, shown in Fig. 1.1 (a) and (b), consists of a primary radiator backed by a metal ground plane and a partially reflecting superstrate (PRS) placed at a cavity height h from the ground plane. The electromagnetic wave which is excited by the radiator is partially reflected back by the superstrate surface while the remaining exits out of the PRS. Then the ground plane re-radiates all the backward waves back to the PRS. The cavity is carefully designed such that waves emanating from the PRS are in phase giving rise to enhanced radiation in the broadside direction. Fig. 1.1 (a) denotes the simple FPC antenna geometry where reflecting elements are printed only on one side of the superstrate layer whereas 1.1 (b) denotes the same with reflecting elements printed on both the sides of the superstrate layer.

In order for the waves leaving the PRS to superpose in phase, the total phase shift of the electromagnetic waves should be an integer multiple (N)

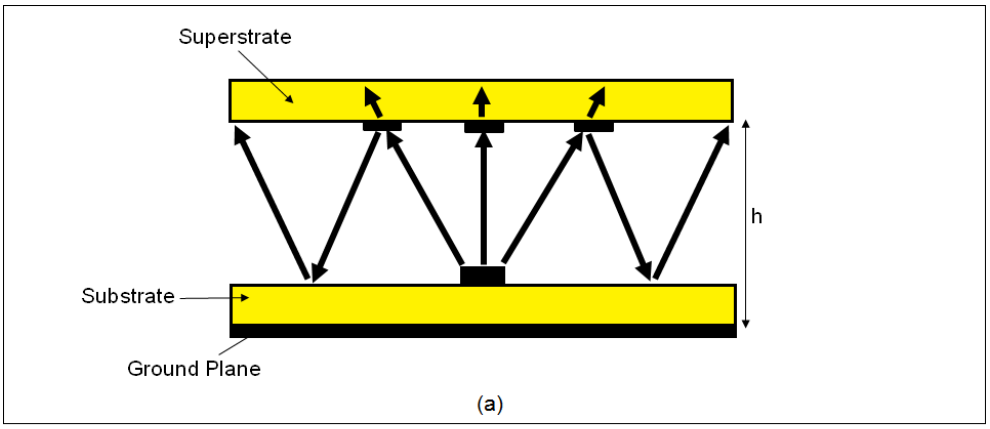

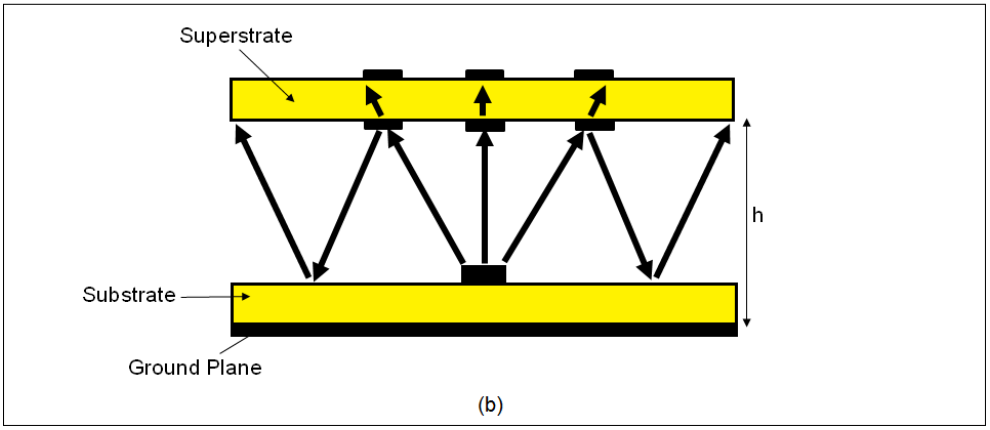

Figure 1.1: Geometry of a simple Fabry Perot cavity antenna with (a)Single-layer printed FSS (b)Double-layer printed FSS. The geometry consists of a primary radiator backed by a ground plate and superstrate layer.

of 2π. Mathematically,

$$-4\pi\frac{h}{\lambda} + \phi_1 + \phi_2 = 2\pi N \tag{1.1}$$

where λ is the wavelength of the source excitation; ϕ_1 and ϕ_2 are the phase shifts introduced by the ground plane and PRS respectively. The resonant frequency of the structure is, therefore, given by

$$f = (\frac{\phi_1 + \phi_2}{2\pi} - N)\frac{c}{2h}, \tag{1.2}$$

where c is the speed of light. The cavity height is designed to be

$$h = (\phi_1 + \phi_2 - 2N\pi)\frac{\lambda}{4\pi}. \tag{1.3}$$

When reflection phase of the ground plane (ϕ_1) and the superstrate layer (ϕ_2) both equal π and $N = 0$, the distance between the ground plane and the superstrate layer is designed to be half wavelength. If one of these plates is replaced by an artificial magnetic conductor that has zero reflection phase, the distance reduces to quarter wavelength [3, 4]. If the cavity is designed such that the ϕ_1=-ϕ_2, then theoretically cavity height h is reduced to zero. Since metamaterials are dispersive, their reflection phase depends on frequency, causing cavity height to also vary [3].

The minimum half-power beamwidth of FPC antenna achieved near the resonant frequency is given by

$$\Delta\Theta_{3dB,min} \simeq \sqrt{\frac{2}{Q}}, \tag{1.4}$$

where Q is the quality factor of the FPC antenna [5]. The directivity is a function of primary source location and the structure of the superstrate. The product of maximum transmitted power ($|T|^2_{max}$) and bandwidth (BW) of an FPC antenna is a function of PRS reflection coefficient r and p, a constant determined by the position of the primary radiator [5, 3]. Mathematically,

$$|T|^2_{max}BW = p\frac{1+|r|}{1-|r|}\frac{2}{\pi}\frac{1-|r|}{\sqrt{r}} \geq \frac{4p}{\pi}. \tag{1.5}$$

1.2 Model of Fabry Perot cavity Antenna

1.2.1 Electromagnetic Band Gap Antenna

FPC antenna may be regarded as a type of electromagnetic bandgap (EBG) resonator antenna with defect mode [6]. EBG materials are formed from one, two or three dimensional periodic dielectric structures [7]. When irregular components are present in the periodic structure creating defects,

localized frequency windows are displayed within the forbidden frequency band where surface waves present at the interface between the substrate and the dielectric do not propagate [8]. The electromagnetic field distribution is altered by the superstrate at the defect frequency and enhanced in a particular direction. These phenomena are responsible for improving the antenna directivity when the EBG structure is used as a superstrate for it [9, 10].

1.2.2 Transmission line model

Transmission line model can be used to analyze the FPC antenna. An FPC antenna where a Hertzian electric dipole is placed above the substrate with $N-1$ superstrate layers, as shown in Fig. 1.2 (a). An equivalent transmission line model was developed where each layer was modeled as a transmission line of different length L_k, $k = 1, 2...N$ and characteristic impedances as Z_{ck} [11]. The first layer ($k = 1$) and N^{th} layer refer to the substrate and the topmost superstrate respectively. The transmission lines, corresponding to the different layers, are cascaded together, as shown in Fig. 1.2 (b). The two nodes K_+ and K_- constitute a k^{th} port. The current and voltages of the k^{th} port are I_k and V_k respectively.

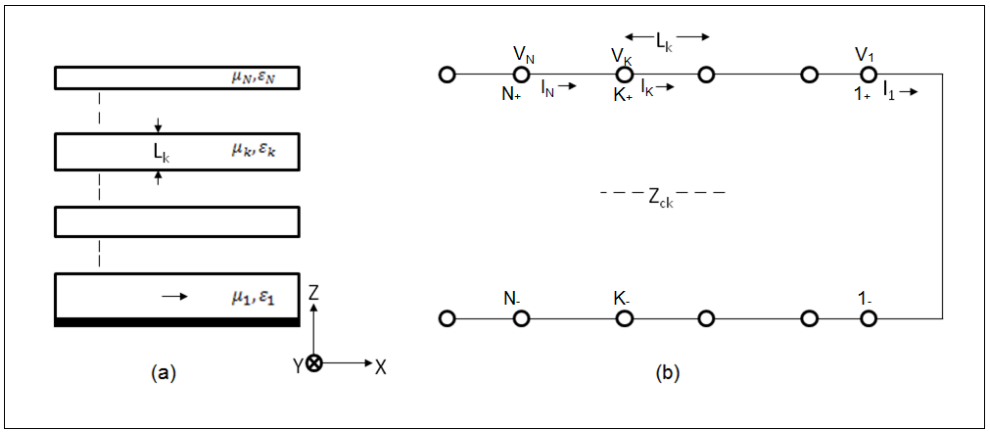

Figure 1.2: Figure showing (a) an FPC antenna with Hertzian electric dipole embedded in substrate with multiple superstrates.(b) Equivalent transmission line network.

1.2.3 Leaky Wave Antenna

Another model of an FPC antenna is a leaky-wave antenna which consists of parallel plate waveguide structures where the top plate is replaced with some sort of leaky partially reflecting surface. The radially propagating mode in the leaky wave antennas is a fast wave where propagation

wavenumber (k) is complex and is given by

$$k = \beta - j\alpha. \tag{1.6}$$

Here α and β are the attenuation and phase constant, respectively. The propagation wave number is complex due to leakage of the power along the structure as the wave propagates. A weakly attenuated leaky-wave (that has small attenuation constant) is dominant in the waveguide structure and can be considered as a source creating large aperture distribution which ultimately results in high directivity of the antennas [3].

1.3 Literature Survey of FPC Designs

FPC antenna was first fabricated in 1956 [12]. The structure consisted of a waveguide aperture on the ground plane and a PRS separated by a half-wavelength thick dielectric substrate. The PRS was formed by parallel metal wires or strips. However it is tedious to design such an FPC antenna in practice. Other experiments were performed in [13] and [5], where a thick dielectric sheet substituted the PRS and was still kept at approximately half-wavelength distance from the ground plane. Later, several layers of dielectric sheets were used as PRS [14]. However, since dielectrics are lossy materials, introduction of multiple dielectrics in the superstrate layer decreases the overall efficiency of the antenna. There exists a trade-off between the operational bandwidth and gain of an FPC antenna [3, 12]. Various ways have been demonstrated to mitigate this challenge. A single layer frequency selective surface (FSS) superstrate was designed as the PRS. An FSS consists of multiple unit cells. In [15], the unit cells were designed with tapered size patches to compensate for phase shifts caused by different path lengths from the rectangular patch radiator to each individual unit cell of the FSS as shown in Fig.1.3. This compensation of phase shifts ensured that all the reflected wave from the PRS have the same phase. The condition of forward radiation is enhanced by means of in-phase bouncing which enhances gain. It was shown that FSS with tapered size patches exhibit higher impedance bandwidth, peak directivity and lower side lobe levels than that of FSS with uniform size patches.

FPC antenna can also be used in beamforming typically used in communication systems. In [16], antenna beam shaping was performed by shifting the primary radiator from the cavity center. A compact steerable FPC antenna was proposed in [17] which consisted of phase varying PRS placed at a distance h from the patch antenna on substrate backed by a ground plane. In a phase varying PRS, the reflection phase varies with the frequency. The PRS reflector consisted of a periodic array of copper strips in the unit cell. To make the antenna beam steerable, the non-uniform gap spacing between the unit cells was employed.

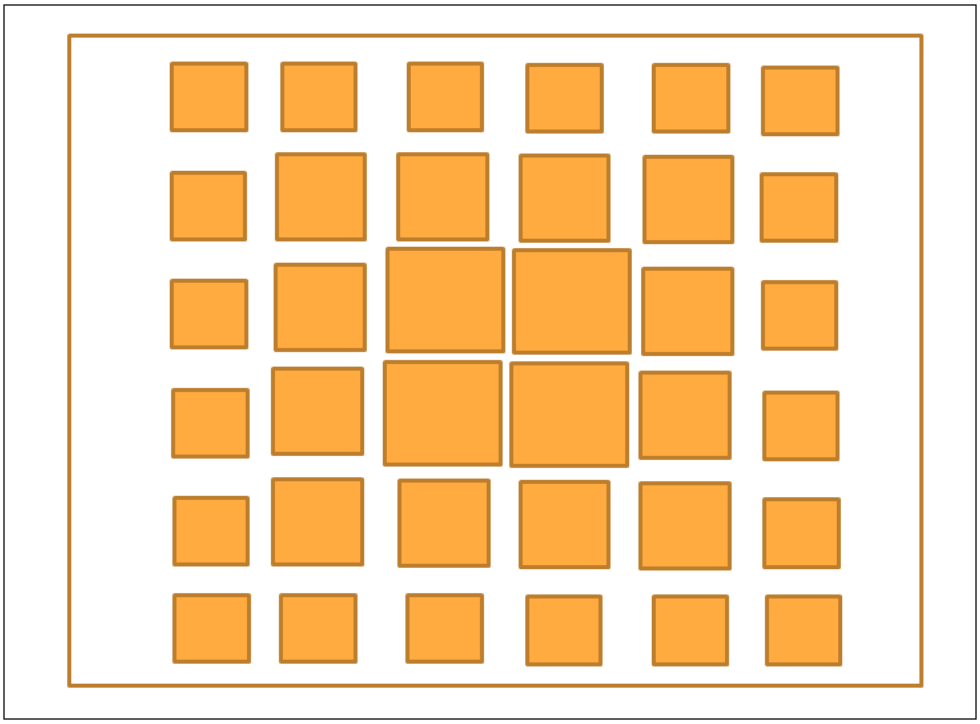

Figure 1.3: Tapered FSS structure with square elements in the unit cell

All the FPC antennas, discussed above, are of linear polarization. In some applications involving mobile users, circular polarization is required to eliminate the possible polarisation mismatch between the transmitted and received signals. This ensures that the receiver antenna receives maximum power from the transmitter antenna irrespective of both the antenna orientations. In other words, the need for alignment of transmitter and receiver antenna for the receiver to receive maximum power gets eliminated.

To achieve a circular polarization with a primary radiator such as patch antenna, a feed point at a particular position on an asymmetric patch could be used. However, this technique is more prone to tolerance errors and has a narrow bandwidth. Another method is to use two orthogonal feed points fed with a 90° hybrid [18, 19]. However, it introduces fabrication complexity in the feeding network leading to issues in cost and efficiency, particularly for applications in the millimeter-wave range [2]. One method for overcoming this limitation is by using a linearly polarized primary radiator. The polarization is subsequently changed to circular by a PRS design. For example, in [20], a low-profile circularly polarized FPC antenna was proposed with a linearly polarized diagonally tilted microstrip patch and integrated with the non-standard artificial magnetic conductor. An artificial magnetic conductor is a type of material which acts as a perfect magnetic conductor (PMC)

over a small frequency range [21]. It has a nearly zero reflection phase at the operating frequency. However, the non-standard AMC employed in [20] had non zero reflection phase of 45° and -45° in the two orthogonal directions of the plane. The superstrate layer consists of a unit cell array containing a square lattice with two orthogonal slots. A circularly polarized antenna using FPC configuration was proposed in [2] where a single layer polarising FSS was placed over a linearly polarized source on a corrugated ground plane. The corrugations were introduced to control the reflection phase at the ground plane. The circular polarization was realized using two orthogonal slots of perpendicular length which were designed in such a way that the resonant frequency of one of the slots was below operating frequency and that of the other slot was above the operating frequency. In [22], a circularly polarized FPC antenna was designed with a metasurface as the superstrate layer. The metasurface consisted of a unit cell array where each unit cell consists of a rectangular loop with a diagonal microstrip embedded inside it. The source antenna was placed at a distance of about 1/17 λ_0 (where λ_0 is the operating wavelength in free space) from the superstrate. Both a patch and slot antenna were used in this paper as the primary radiators resulting in significant increase in return loss bandwidth and substantial improvement in the axial ratio. A broad bandwidth was achieved along with wide gain and axial ratio bandwidth. A compact FPC antenna with metasurface containing double annular slot resonator with spikes in the unit cell shown in Fig.1.4 was proposed in [23]. The antenna resulted in high gain enhancement of the patch antenna.

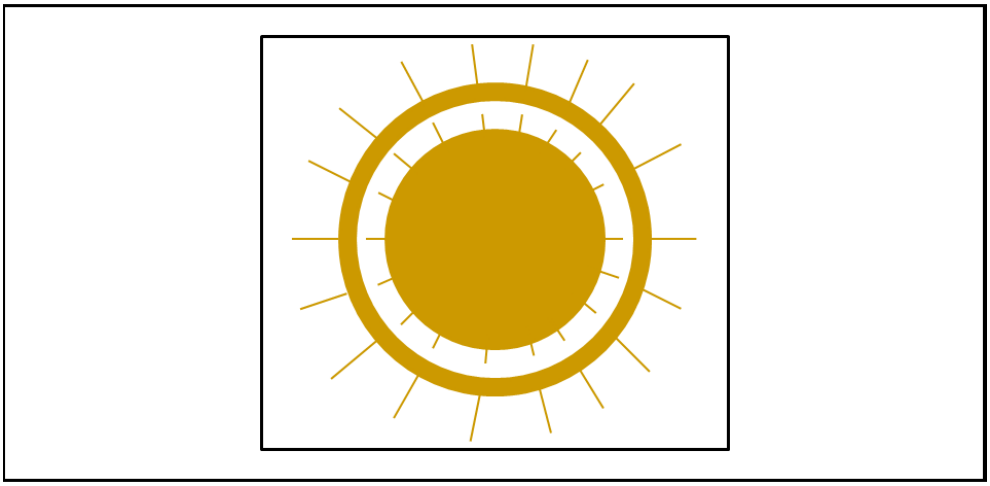

Figure 1.4: Spiked double annular slot resonator

In our thesis, we examine a new method for improving antenna characteristics. We study the impact of introducing roughness in the unit cell elements. The roughened surface generally refers to the serrations intro-

duced around the periphery of the surface. The degree of roughness is given by the number of serrations around the periphery of the element. This concept is illustrated in Fig. 1.5. Fig. 1.5 (a) and (b) denote the roughened

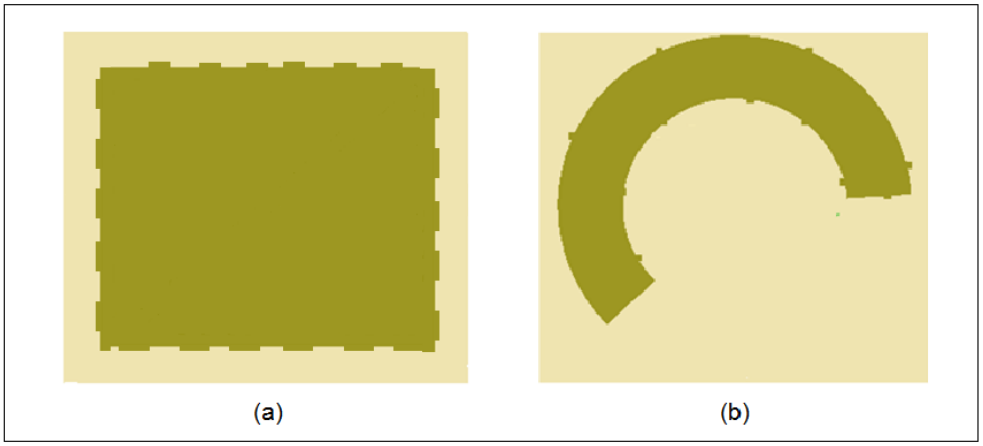

Figure 1.5: Roughness around the periphery of a (a) square element and (b) arc design.

square element and the arc in the unit cell respectively. We have considered two different units: an arc and rectangular loop with a diagonal element. In both the unit cells, we have introduced roughness in the unit cell elements in the superstrate layer and obtained simulated return loss bandwidth, gain, and axial ratio for these designs, as discussed in Chapter 3 and 4.

1.4 Thesis objectives

The problem statement in this thesis consists of the following:

- Design of two types unit cells - arc and rectangular loop - with peripheral roughness, in the superstrate PRS layer of an FPC antenna.
- Examine the effect of unit cell design on antenna properties such as gain, bandwidth and axial ratio.

1.5 Thesis outline

This thesis is organized in the following manner. In Chapter 2, the design of the primary radiator, the patch antenna, is discussed. Chapter 3 discusses the design of the metasurface containing circular arc in the unit cell. The arc design parameters and the effect of roughness along the arc periphery on the return loss bandwidth, gain, and the axial ratio are discussed. Chapter 4 discusses the FPC antenna with metasurface containing

rectangular loop with the diagonal in the unit cell. Effect of design parameters of the rectangular loop along with peripheral roughness on the return loss bandwidth, gain, and the axial ratio are discussed in detail. Chapter 5 briefly summarizes the results obtained in this thesis, limitations, and future work.

Chapter 2

Design of Primary Radiator: Patch Antenna

This chapter discusses the design of the patch element as the primary radiator of the FPC antenna. The general side view structure of the FPC antenna is shown in Fig. 2.1. This figure shows the bottom layer with a

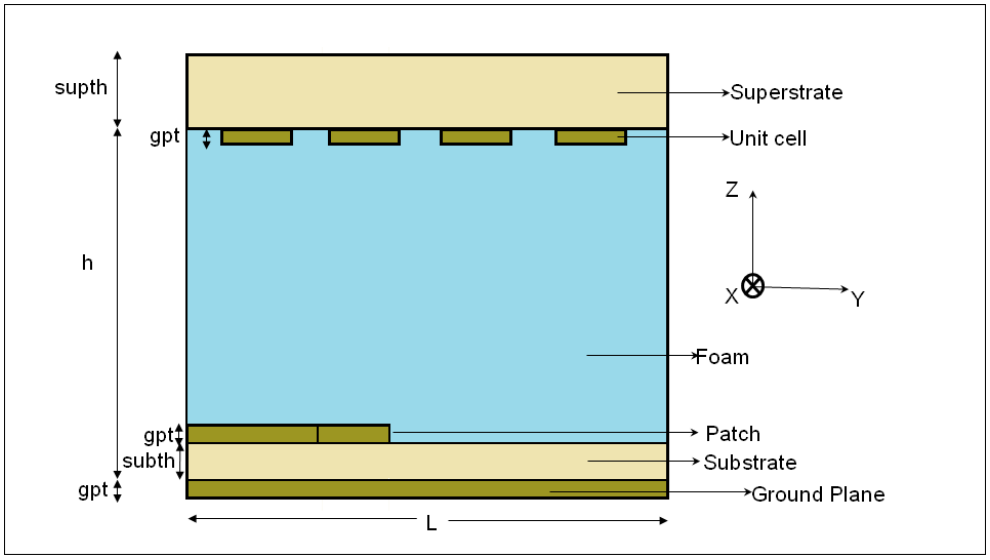

Figure 2.1: Side view of proposed Fabry Perot cavity(FPC) antenna containing arc in the unit cell placed beneath the superstrate layer. The substrate is Rogers RO4350B while the unit cells are of copper. The foam is made of thermocol.

patch element, of thickness *gpt*, as the primary radiator. The patch has a single feed and is backed by a substrate layer, of thickness *subth*, followed by ground plane, also of *gpt* thickness. A foam of $h - subth$ thickness is mounted above the patch element and followed by the partial reflecting

surface consisting of an array of metallic unit cells followed by a dielectric superstrate of *supth* thickness. We have chosen Rogers RO4350B laminate as both the substrate and the superstrate layers. The foam is made of thermocol of dielectric constant = 1.05 and provides mechanical support to the latter. This design is modeled in CST Microwave Studio 2018.

2.1 Methodology

We have first designed a simple patch at a resonant frequency of 2.45 GHz. The length and width of the patch and the feed were tuned individually to obtain the desired resonant frequency. A two-stage quarter-wave transformer was used to impedance match the patch to a coaxial feed of 50Ω as shown in Fig.2.2. The widths of the quarter wave transformer are $fw1$, $fw2$ and $fw3$ and their lengths are $fl1$, $fl2$ and $fl3$. The length and width of the patch are pl and pw, respectively. The thickness of both the ground plane and the patch is denoted by gpt. The thickness of the substrate is given by $subth$. The top view of a simple patch antenna is shown in Fig. 2.2. The

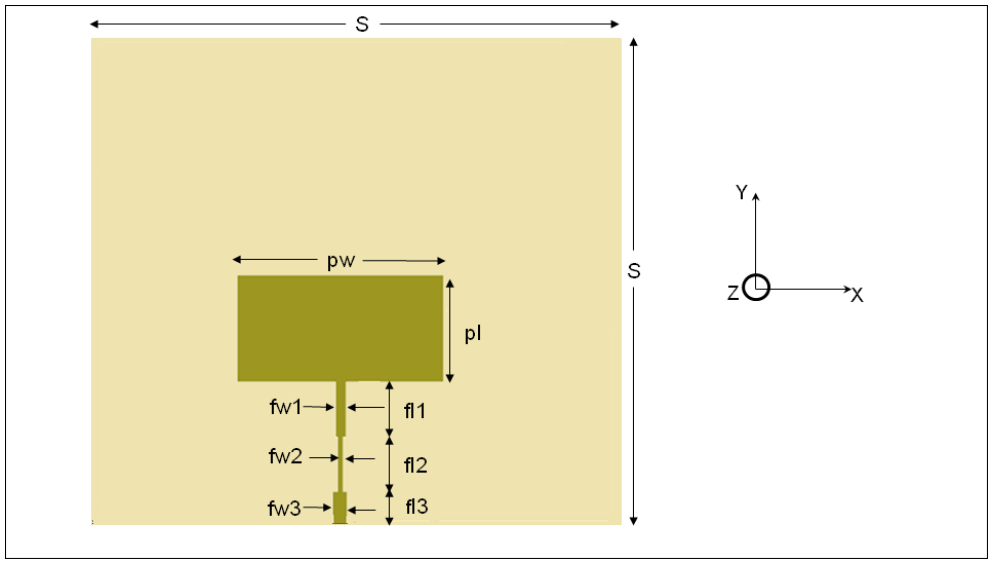

Figure 2.2: A simple patch antenna on Rogers RO4350B substrate of thickness 0.76mm. The patch was designed at resonant frequency of 2.45 GHz. The dimensions of the patch are $pl \times pw$. A two-stage quarter-wave transformer is employed for the patch design. The widths of the three feeds shown in the figure are $fw1$, $fw2$ and $fw3$. The lengths of the three feeds are $fl1$, $fl2$ and $fl3$.

parameters of the patch design are shown in Table 2.1.

Table 2.1: List of parameters for the simple patch antenna dimensions

Patch Dimensions	Values(mm)
pl	33
pw	63
$fl1$	17
$fl2$	17
$fl3$	9.5
$fw1$	2.89
$fw2$	1.633
$fw3$	4.65
$subth$	0.762
gpt	0.035
L	120

2.2 Results

Fig. 2.3 (a)-(c) depict the simulated return loss, gain and the axial ratio for the simple patch antenna respectively. The patch had return loss bandwidth of 20 MHz (0.82%), a low gain of 3.378 dBi at the resonant frequency of 2.45 GHz and a very high axial ratio indicating linear polarization.

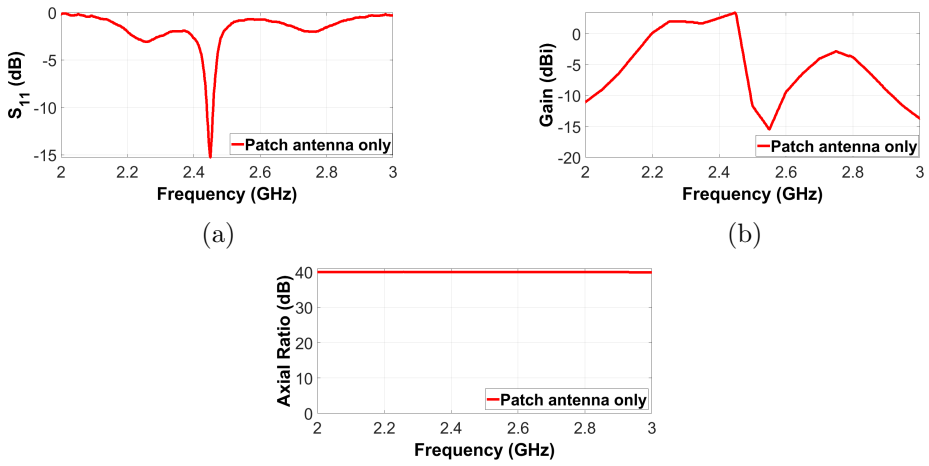

(a) (b) (c)

Figure 2.3: Simulation results for the simple patch antenna: (a) Return loss, (b) Gain, (c) Axial Ratio.

Chapter 3

Design of Metasurface Superstrate: With Arc in the Unit cell

This chapter discusses the design of both smooth and rough arcs in the unit cell in the superstrate layer of the FPC antenna shown in Fig. 2.1 of the previous chapter. The metasurface superstrate was placed at a cavity height h of $6.05mm$ from the ground plane. The superstrate is designed to have a 4×4 array of identical unit cells of length ($ll = 26.25mm$) and width ($lw = 24.5mm$). Each unit cell consists of an arc whose design is based on variation of four parameters: starting angle (pi), ending angle (pf), radius of the inner circumference of arc (r) and arc thickness (at) as shown in the Fig.3.1. The radius of the inner circumference of the arc was randomized between $0.2mm$ and $4mm$. Starting angle pi and the angular span of the arc were randomized between $0°$ to $360°$. Ending angle pf was calculated by adding the angular span to the initial angle. If the final angle exceeded $360°$, then $360°$ was subtracted from the maximum angle. In this process, if the ending angle was smaller than the starting angle, then their values were swapped so that the ending angle always remained greater than the starting angle. The circular arc thickness at was randomized between $1mm$ to $6mm$. Hundred different designs of circular arc were designed for the unit cell on the basis of variation of these parameters.

We obtained results for simulated return loss, gain, and axial ratio for each of these antennas. Histograms depicting return loss bandwidth, gain and axial ratio variations for these designs are shown in Fig. 3.2 (a)-(c) respectively. From Fig.3.2 (a), we infer that the maximum, minimum and the mean bandwidths with relative bandwidths in brackets are 229.02 MHz (10.01%), 2.29 MHz (0.15%), and 36.54 MHz (1.48%) respectively. The numbers in the brackets indicate the relative bandwidths of the antennas. The relative bandwidth is the ratio of the bandwidth over the resonant

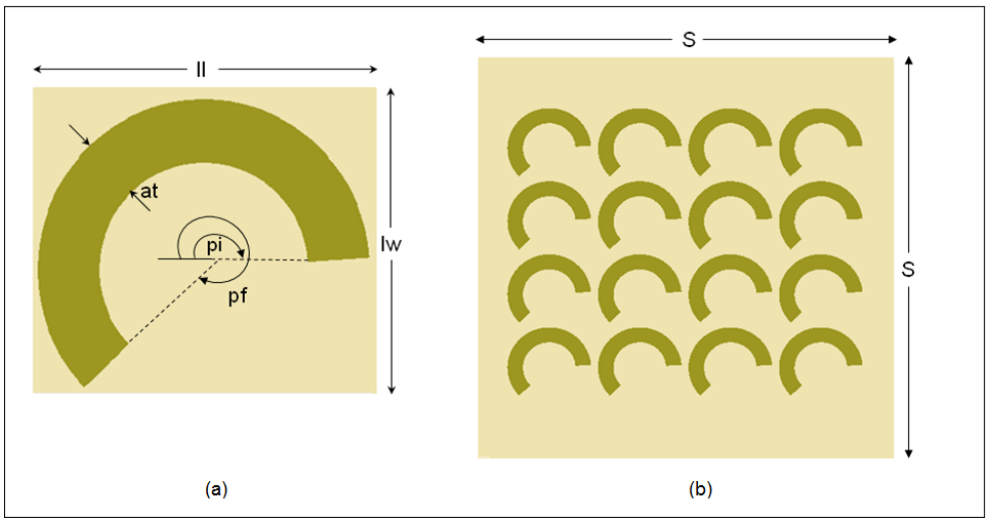

Figure 3.1: (a) Arc design in the unit cell with the four design parameters: starting angle (pi), ending angle(pf), radius of the inner circumference of arc (r) and arc thickness (at). (b) 4×4 arrangement of unit cells containing smoothened metasurface on the superstrate layer.

frequency. The maximum, minimum, and the mean gains are 8.95 dBi, -8.98 dBi and 2.94 dBi respectively. The maximum, minimum, and the mean axial ratios are 40 dB, 7.46 dB, and 26.64 dB respectively. Fig. 3.3 (a)-(c) show the unit cell arc design in the superstrate layer for which the maximum and minimum bandwidth, gain and axial ratio were obtained. Table 3.1 summarizes the arc parameters for the maximum and minimum return loss bandwidth, gain and axial ratio of the FPC antenna. The FPC antenna with arc design in the superstrate layer that gives rise to the minimum axial ratio of 7.46 dB and gain greater than that of the patch was chosen for the analysis in further sections, as shown in Fig.3.4 (a). The 4×4 arc array in the metasurface superstrate layer is shown in Fig.3.4 (b).

Table 3.1: List of arc design parameters in the unit cell

	Radius $r(mm)$	Arc thickness $at(mm)$	Starting angle $pi(^\circ)$	Ending angle $pi(^\circ)$
Maximum Bandwidth	1	5	86°	238°
Minimum Bandwidth	3	3	175°	209°
Maximum Gain	1	5	86°	238°
Minimum Gain	0.5	6	86°	206°
Maximum Axial Ratio	0.5	6	81°	281°
Minimum Axial Ratio	1	4.5	176°	316°

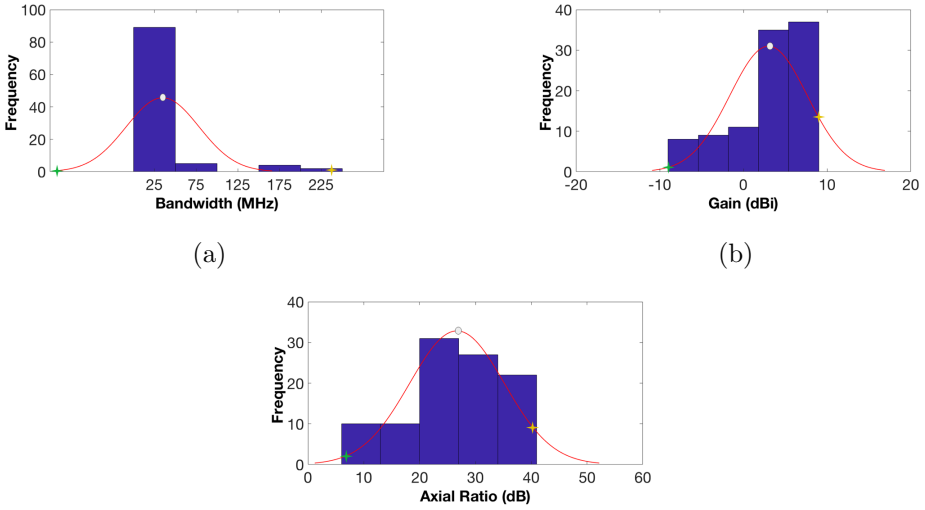

(a) (b) (c)

Figure 3.2: Histogram depicting variations for hundred different designs of smooth arcs in the superstrate layer over (a) bandwidth, (b) gain and (c) axial ratio. The peak of the red curve denotes the mean.

3.1 Effect of cavity height on bandwidth, gain and axial ratio of FPC cavity antenna with metasurface containing smooth arc in the unit cell

To understand the effect on return loss bandwidth, gain and axial ratio on varying cavity height h, we performed a parameter sweep for the cavity height from $3mm$ to $6mm$ with a step size of $0.5mm$. The plots for bandwidth, gain and axial ratio versus h are shown in Fig. 3.5 (a)-(c) respectively.

From Fig. 3.5 (a), we note that the bandwidth of the FPC antenna increases drastically from $h = 3mm$ to $5.5mm$. However, after $5.5mm$, the bandwidth starts to decrease. Maximum and minimum bandwidth with relative bandwidth in brackets is 30.91 MHz (1.21%) and 21.84 MHz (0.89%) for a cavity height of $5.5mm$ and $3mm$ respectively. From Fig. 3.5 (b) gain decreases up to cavity height value of $3.5mm$, and after $3.5mm$ on wards, gain starts to increase. The maximum and minimum gain is 5.19 dBi and 2.56 dBi at a cavity height of $6mm$ and $3.5mm$ respectively. However, axial ratio value decreases almost linearly with an increase in cavity height (h) as depicted in Fig. 3.5 (c). The maximum and minimum axial ratio is 30.53 dB and 7.78 dB for the cavity height of $3mm$ and $6mm$ respectively. After studying these variations, we chose the cavity height(h) as $6.05mm$.

Fig. 3.6 (a)-(c) compare the simulated return loss, gain and axial ra-

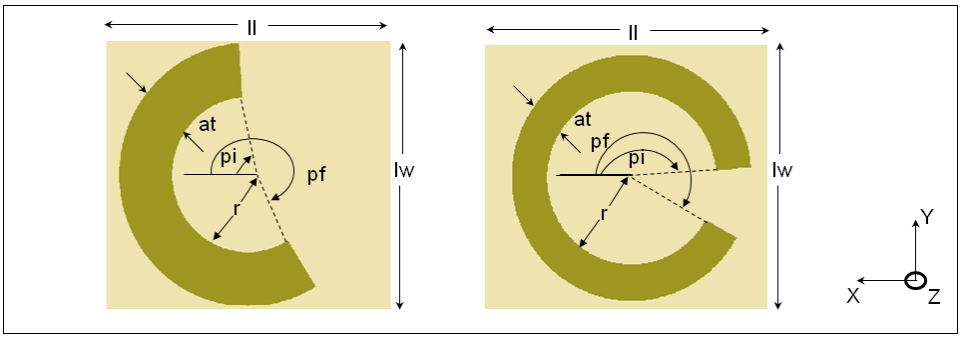

(a)

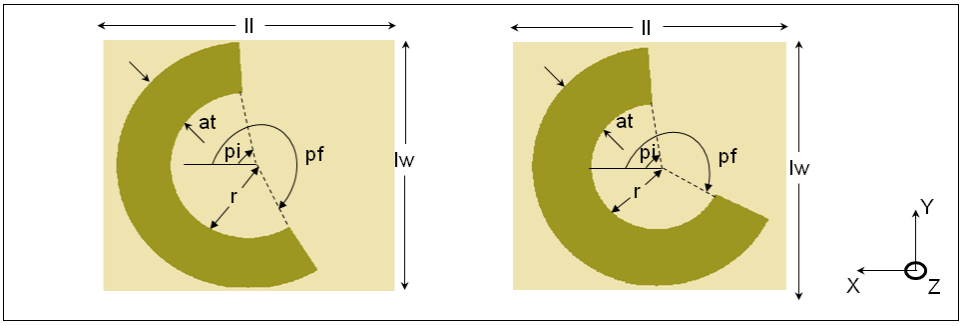

(b)

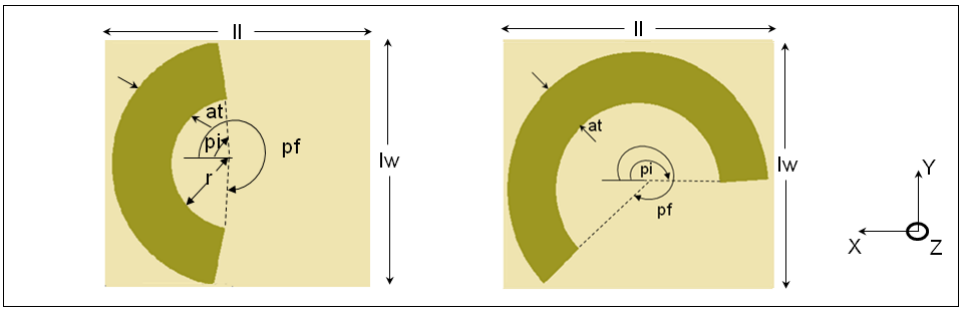

(c)

Figure 3.3: Arc design in the unit cell in the superstrate layer depicting (a) maximum and minimum bandwidths respectively, (b) maximum and minimum gain respectively, and (c) maximum and minimum axial ratios respectively.

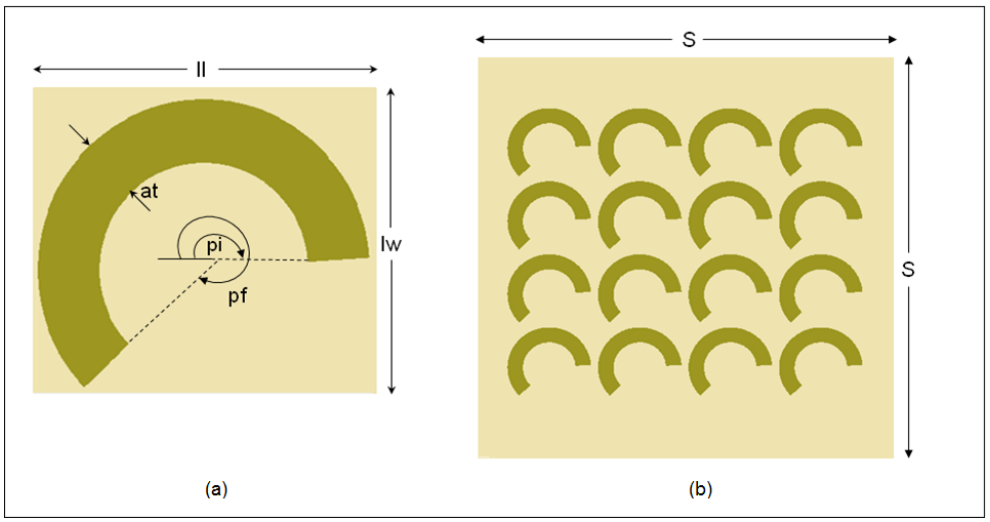

Figure 3.4: (a) Arc design in the unit cell designed for minimum axial ratio. (b) 4×4 arrangement of unit cell containing smoothened arc in the metasurface superstrate layer.

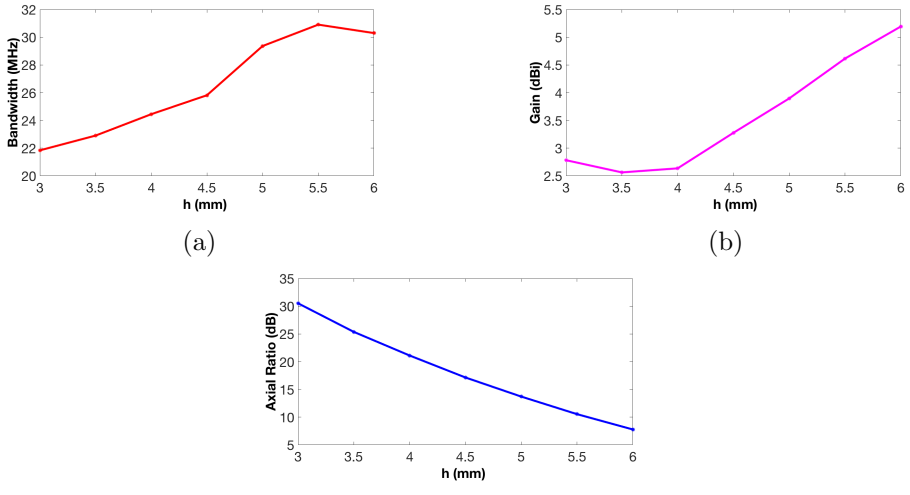

Figure 3.5: Plot showing the effect of cavity height h on (a) bandwidth (b) gain (c) axial ratio

tio of the patch and FPC antenna with 4×4 arc array in the metasurface superstrate layer. The latter is hitherto referred as FPCMA. We observe that the bandwidth of the latter is enhanced slightly after introducing superstrate layers above the primary radiating source. The bandwidth of the patch antenna and FPCMA are 20 MHz (0.816%) and 31.21 MHz (1.29%) respectively while their resonant frequencies are 2.45 GHz and 2.43 GHz

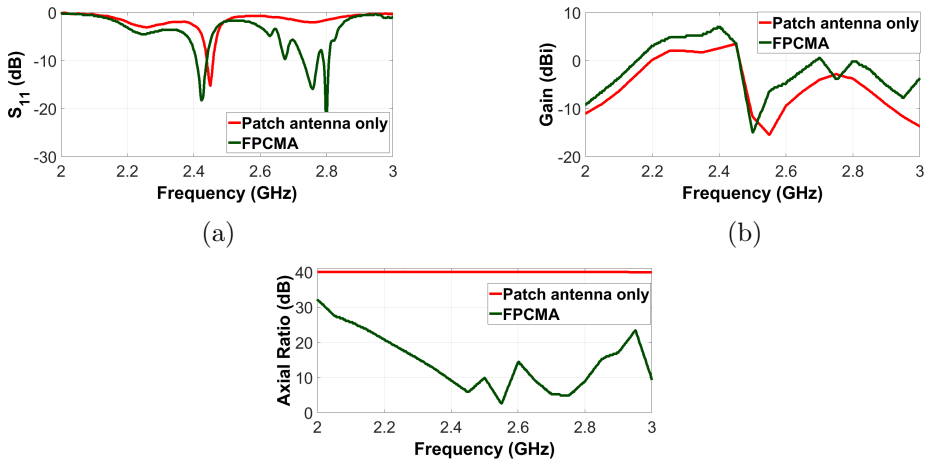

Figure 3.6: Comparison of simulated results for a simple patch antenna and FPC antenna with metasurface containing arc(FPCMA): (a) return loss (b) gain (c) axial ratio.

respectively. From Fig.3.6 (b), it is observed that the gain for a simple patch antenna at a resonant frequency of 2.45 GHz is 3.38 dBi. From Fig. 3.6 (c), we observe that the axial ratio for the simple patch antenna is high indicating that the patch is linearly polarized. However, after introducing the superstrate layer with arc embedded below it at a cavity height h from the ground plane, we see that the axial ratio at the resonant frequency of 2.43 GHz has significantly reduced to 7.46 dB.

3.2 Rough Arcs

Roughness was introduced in the arc in the unit cell by introducing thirteen small bricks around the periphery of the arc. The positions of the bricks were varied randomly along the periphery of the arc using MATLAB software. Hundred such designs of roughened arc were generated and the return loss, gain, and axial ratio were simulated. A histogram was then performed to obtain various distributions for these parameters and identify the mean bandwidth, gain, and axial ratio. Fig. 3.7 (a)-(c) depict the roughened arc design in the unit cell depicting maximum and minimum return loss bandwidth, gain and axial ratio respectively.

Fig. 3.8 (a)-(c) depict the histogram distributions for the return loss bandwidth, gain and axial ratio. As seen in these figures, the green and yellow star denote the minimum and maximum return loss bandwidth, gain and axial ratio respectively out of all hundred different roughness designs. The peak of the red curve denotes the mean parameter of all the hundred designs

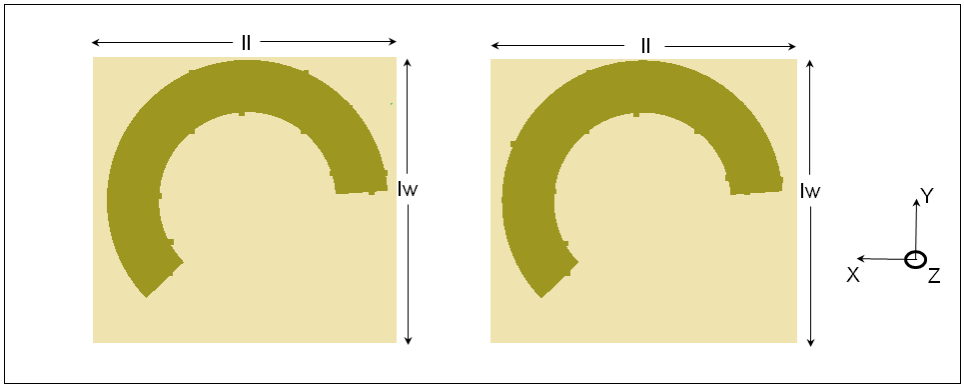

(a)

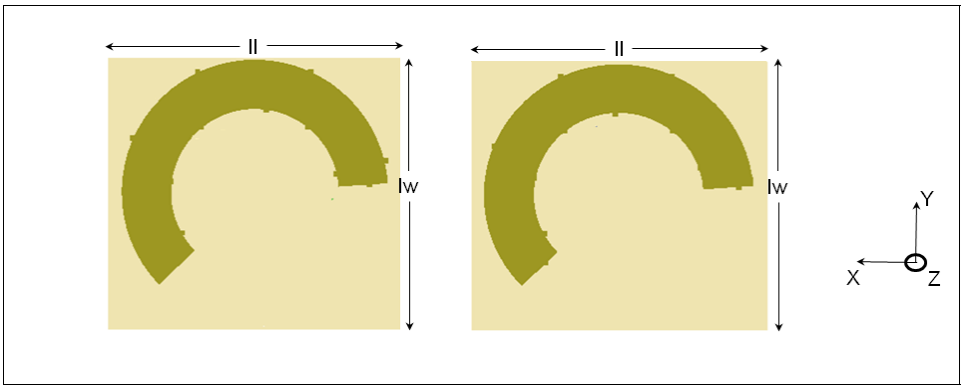

(b)

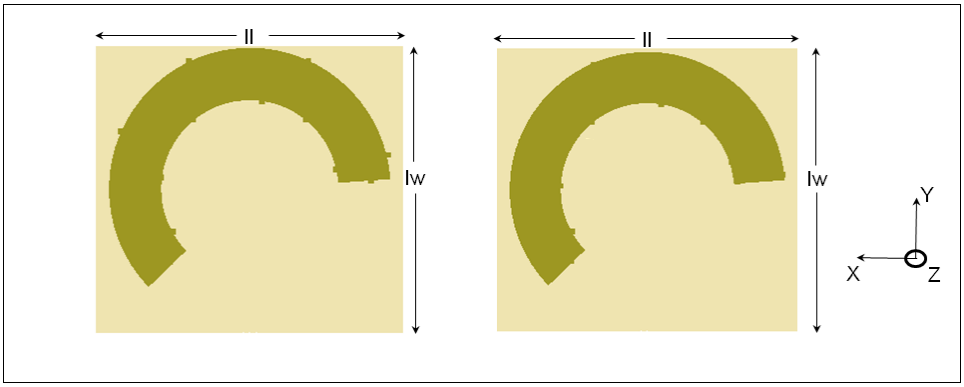

(c)

Figure 3.7: Rough arc design in the unit cell in the superstrate layer depicting (a) maximum and minimum return loss bandwidth respectively, (b) maximum and minimum gain respectively, and (c) maximum and minimum axial ratios respectively.

for the roughened arc. The maximum, minimum, and mean bandwidth of FPC antenna is 36.07 MHz(1.49%), 17.12 MHz(0.71%), and 31.59 MHz (1.3%) respectively. The maximum, minimum and mean gains of the FPC antenna with roughened metasurface designs are 5.72 dBi, 5.05 dBi, and 5.39 dBi respectively whereas the maximum, minimum and the mean axial ratios are 9.09 dB, 6.84 dB, and 7.90 dB respectively. Even after introducing roughness in the arc in the superstrate layer, the minimum axial ratio was 6.84 dB.

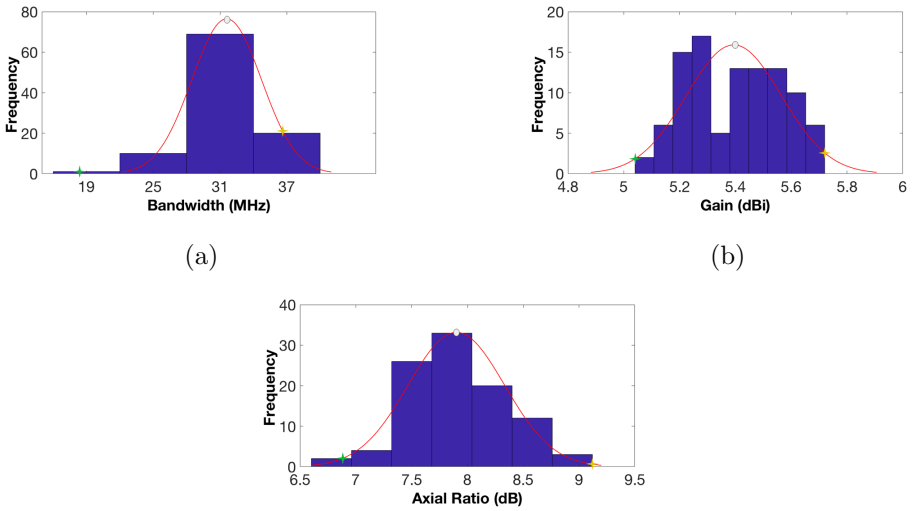

(a) (b)

(c)

Figure 3.8: Histogram depicting variations for hundred different designs of rough arcs in the unit cell in the metasurface superstrate layer over (a) bandwidth, (b) gain and (c) axial ratio. The peak of the red curve denotes the mean of all the hundred designs in the FPC antenna.

Chapter 4

Design of Metasurface Superstrate: With Rectangular Loop with Diagonal in the Unit cell

This chapter discusses the design of a unit cell in the metasurface superstrate layer consisting of either a smooth or rough rectangular loop with a diagonal. The effect of the variation of the design parameters on the return loss bandwidth, gain and the axial are discussed in detail.

4.1 Methodology

On the patch antenna with specifications mentioned in chapter 2, the superstrate layer was added with a 4×4 unit cell array, each containing a rectangular loop with a diagonal. To achieve a wide bandwidth, high gain and axial ratio below 5 dB, various design parameters of the metasurface such as the thickness (lt), diagonal ($diag$) of the rectangular loop, length (ll) and width (lw) of the unit cells and cavity height (h) were tuned individually as shown in Fig.4.1.

4.2 Study of effect of various metasurface design parameters on return loss bandwidth, gain and axial ratio

Fig. 4.2 (a)-(c) depict the effect of varying the unit cell length (ll) on return loss bandwidth, gain and axial ratio. During this process, we kept the unit cell width (lw) as $22mm$. Parametric sweep is performed for unit cell length (ll) from $23.5mm$ to $29mm$ with a step size of $0.5mm$. We observe

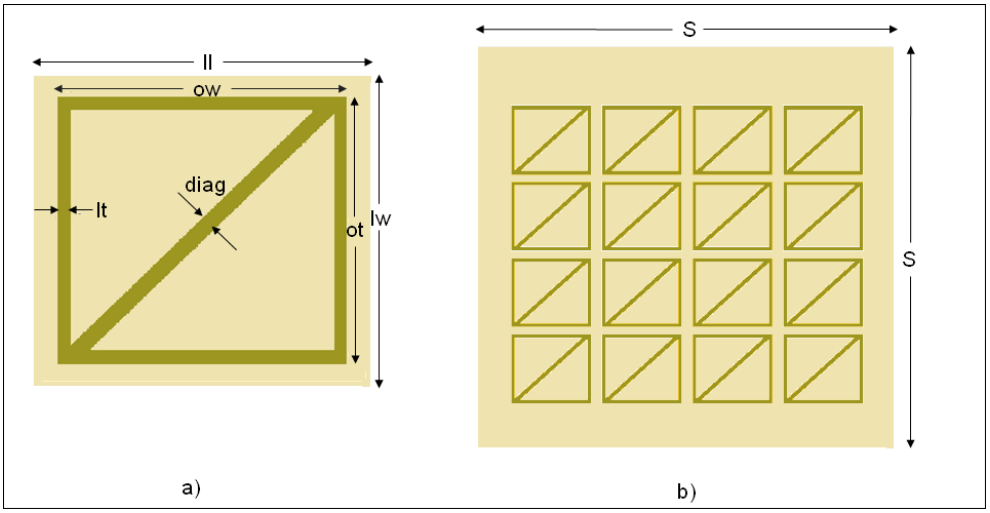

Figure 4.1: (a) Rectangular loop with the diagonal in the unit cell, (b) Metasurface superstrate containing 4×4 arrangement of such unit cells.

a minimum bandwidth of 78.30 MHz (3.41%) at $28mm$. Gain remains nearly constant up to $26mm$ but starts decreasing afterward. The maximum and minimum gains are 9.48 dBi and 8.47 dBi at the unit cell length of $25.5mm$ and $28.5mm$ respectively. There is a nearly linear decrease in axial ratio when unit cell length is increased up to $28mm$ but starts increasing afterward. The maximum and minimum axial ratios obtained are 15.64 dB and 3.73 dB at the unit cell length of $23.5mm$ and $28mm$ respectively.

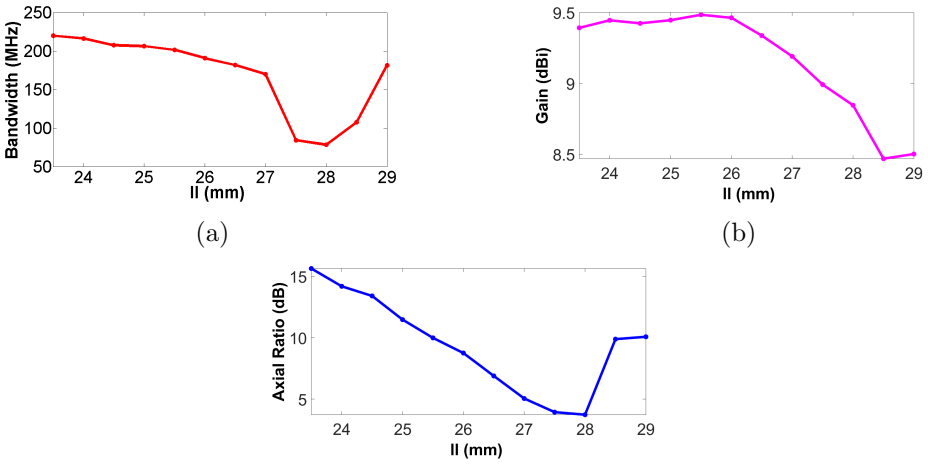

(a) (b) (c)

Figure 4.2: Plot depicting effect of unit cell length (ll) on: (a) bandwidth, (b) gain and (c) axial ratio.

Fig. 4.3 (a)-(c) depict the effect of unit cell width (lw). During this process, we fixed the unit cell length (ll) to $26.25mm$. Parametric sweep is performed for unit cell width lw from $22mm$ to $28mm$ with a step size of $0.5mm$. We observe overall fluctuation in the bandwidth while varying unit cell width lw. There is a sharp decrease in the bandwidth of the FPC antenna when the unit cell width lw is increased from $22.5mm$ to $23mm$. We observe fluctuation in bandwidth when it is varied from $23.5mm$ to $24.5mm$ and this increases up to a unit cell width of $27mm$. The bandwidth starts to decrease again after increasing the unit cell width(lw) beyond $27mm$. The maximum and minimum bandwidths obtained are 187.39 MHz (8.36%) and 9.03 MHz (1.09%) respectively. The gains remain nearly constant up to unit cell width of $23mm$ and a sharp decrease is observed when it is increased from $23mm$ to $23.5mm$. The gain then increases sharply up to the unit cell width of $24.5mm$ and fluctuation is observed when it is increased beyond $24.5mm$. A lot of variation is observed in axial ratio while varying the unit cell width. The maximum and minimum gains observed are 9.42 dBi and -0.02 dBi at the unit cell width of $23.5mm$ and $22mm$ respectively whereas the maximum and minimum axial ratios achieved are 38.18 dB and 6.02 dB for the case of $lw = 25.5mm$ and $23mm$ respectively.

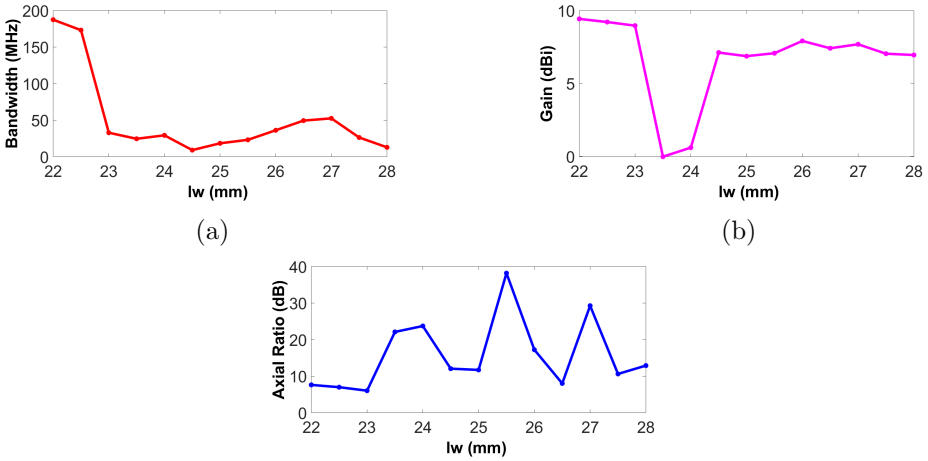

Figure 4.3: Plot depicting the effect of unit cell width (lw) on: (a) bandwidth (b) gain and (c) axial ratio.

Next, we study the effect of rectangular loop thickness lt as shown in Fig. 4.4 (a)-(c) respectively. Loop thickness lt is varied from $1mm$ to $6mm$ with a step size of $0.5mm$. We note that the bandwidth of the FPC antenna first increases when loop thickness is increased to $2mm$ and then starts decreasing on wards in a nearly exponential fashion. The maximum and minimum bandwidths were 226.87 MHz (9.94%) and 42.98 MHz (1.78%)

for the case of $lt = 2mm$ and $6mm$ respectively. Interestingly, the gain and the axial ratio of the FPC antenna are found out to be nearly inversely proportional and proportional to the loop thickness respectively. So, we observe a trade-off between the gain and axial ratio while varying the loop thickness. Maximum and minimum gains are 9.49 dBi and 6.78 dBi at loop thickness of $1.5mm$ and $6mm$ respectively. Maximum and minimum axial ratios are 37.28 dB and 7.54 dB obtained at loop thickness of $6mm$ and $1mm$ respectively.

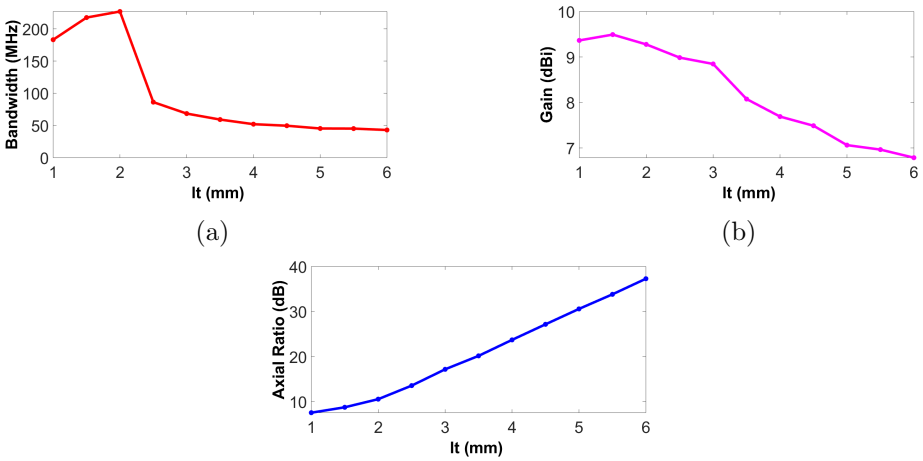

Figure 4.4: Plot depicting effect of loop thickness (lt) on: (a) bandwidth, (b) gain and (c) axial ratio.

We have further investigated the effect of the thickness of the diagonal ($diag$) of the unit cell as shown in Fig. 4.5 (a)-(c). We have performed parametric sweep for $diag$ from $1mm$ to $3mm$ with a step size of $0.5mm$. We note that there is a monotonic increase in both the bandwidth and the axial ratio with the increase in $diag$. The maximum and minimum bandwidths are 215.02 MHz (9.51%) and 179.68 MHz (8.04%) at the diagonal thickness of $3mm$ and $1mm$ respectively. The maximum and minimum axial ratios are 9.48 dB and 7.34 dB at the diagonal thickness of $3mm$ and $1mm$ respectively. However, there is a monotonous increase in gain when the diagonal width is varied up to $2mm$ but starts decreasing when it is increased from $2mm$ to $2.5mm$. The gain then remains nearly constant when the diagonal thickness is increased further from $2.5mm$ to $3mm$. The maximum and minimum gains are 9.55 dBi and 9.32 dBi for diagonal thicknesses of $2mm$ and $1mm$ respectively.

Fig. 4.6 (a)-(c) depict the effect of varying the cavity height h on the return loss bandwidth, gain and axial ratio. The cavity height is varied from $3mm$ to $6mm$ with a step size of $0.5mm$. We observe a nearly lin-

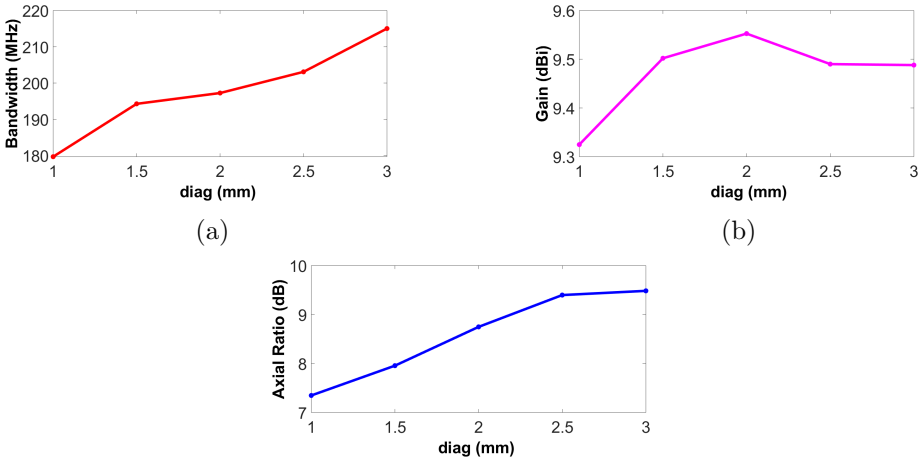

Figure 4.5: Plot depicting effect of diagonal ($diag$) on: (a) bandwidth, (b) gain and (c) axial ratio.

ear increase in bandwidth with an increase in height (h) up to $4.5mm$. The bandwidth increases sharply when the cavity height is increased from $4.5mm$ to $5mm$. However, it starts decreasing slowly when the cavity height is increased beyond $5mm$. The maximum and minimum bandwidths are 208 MHz (10.14%) and 24 MHz (2.96%) at a cavity height of $5mm$ and $3mm$ respectively. We see the monotonic increase in gain throughout on increasing the cavity height. The maximum and minimum gains are 9.43 dBi and 3.43 dBi at a cavity height of $6mm$ and $3mm$ respectively. In the case of axial ratio, there is a sharp increase when the cavity height is varied from $3mm$ to $3.5mm$. There is an approximately linear decrease in the axial ratio when the cavity height is increased beyond $3.5mm$. The maximum and the minimum axial ratios are 19.65 dB and 7.82 dB at the cavity heights of $3.5mm$ and $6mm$ respectively.

After studying all these variations, optimal parameter values were chosen to obtain a minimal axial ratio along with high bandwidth and gain as shown in Table 4.1.

4.3 Results and Analysis

Fig. 4.7 (a)-(c) show the simulated return loss for a simple patch, FPC antenna with metasurface containing arc (FPCMA) and rectangular loop with the diagonal (FPCMRLD) in the unit cell. As we can see, adding the metasurface superstrate layer with the rectangular loop and the diagonal in the unit cell enhanced the return loss bandwidth to 188.51 MHz (8.38%). This is due to the presence of two resonant frequencies at 2.19 GHz and

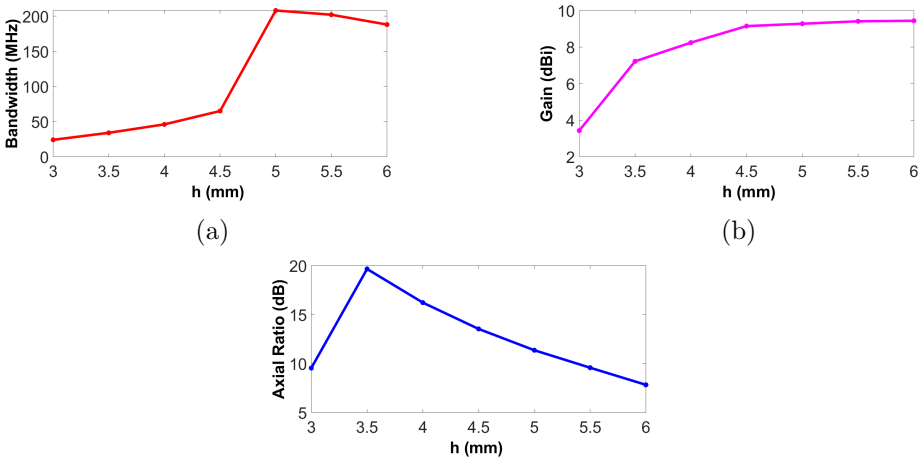

(a) (b) (c)

Figure 4.6: Plot depicting effect of cavity height(h) on : (a) bandwidth, (b) gain, (c) axial Ratio.

2.29 GHz respectively whereas simple patch and FPC antenna with the metasurface containing arc has a single resonant frequency at 2.45 GHz and 2.43 GHz respectively. We observe that gain of FPC antenna with metasurface containing rectangular loop and the diagonal in the unit cell is 9.42 dBi at a resonant frequency of 2.29 GHz whereas the simple patch and FPC Antenna with metasurface containing arc in the unit cell has a gain of 3.38 dBi and 5.18 dBi at the resonant frequency of 2.45 GHz and 2.43 GHz respectively. The axial ratio of FPC antenna with metasurface containing rectangular loop and the diagonal in the unit cell is 7.61 dB at a resonant frequency of 2.29 GHz whereas that of the simple patch and FPC antenna with metasurface containing arc in the unit cell is 40 dB and

Table 4.1: List of parameters for the metasurface dimensions in the superstrate layer

Parameter	Values(mm)
ll	26.25
lw	22
h	6.05
$supth$	1.524
lt	1.05
$diag$	1.26
ow	23.1
ot	19.9

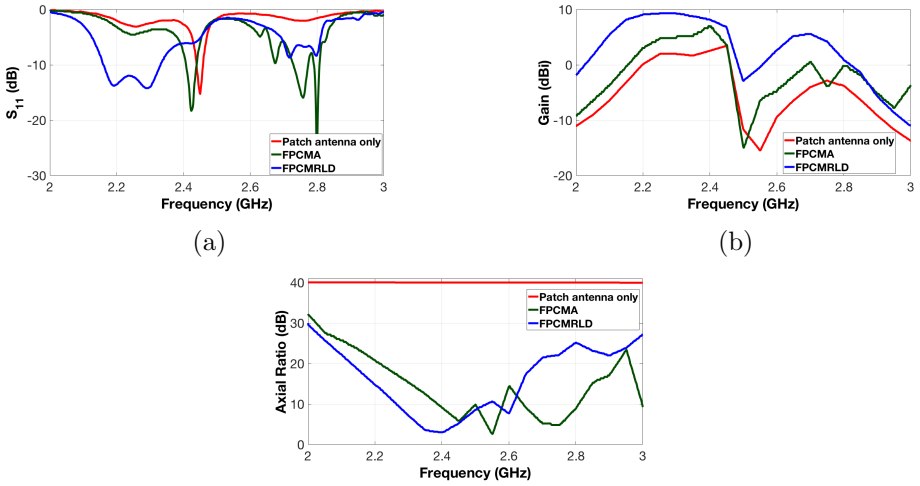

Figure 4.7: Comparison of the simulation results for the simple patch antenna, FPC antenna with metasurface containing arc (FPCMA) and rectangular loop with the diagonal (FPCMRLD) in the unit cell: (a) Return loss, (b) Gain, (c) Axial Ratio.

7.46 dB respectively. Even though the axial ratio of the FPC antenna with metasurface containing rectangular loop and the diagonal is significantly reduced, but the antenna is still linearly polarised. Therefore, the need arose to incorporate roughness in the metasurface to check the effect on its return loss bandwidth, gain, and axial ratio. This is discussed in the next section.

4.4 Analysis of FPC antenna with roughness present in the inner periphery of the rectangular loop and diagonal in the unit cell

We have introduced roughness in the inner periphery of the rectangular loop and the diagonal by introducing thirty six small bricks around them. The position of the brick was varied along them so as to create hundred different designs through randomization of each brick position. In this way, we have generated hundred different positions of these bricks using MATLAB. The return loss, gain and axial ratio for these hundred different designs were simulated. The unit cell designs with roughness only in the inner periphery of the rectangular loop and the diagonal causing maximum and minimum return loss bandwidth, gain and axial ratio are shown in the Fig. 4.8. Fig. 4.9 (a)-(c) shows the histogram for the variation of the return loss bandwidth, gain and axial ratio respectively for the FPC antenna with

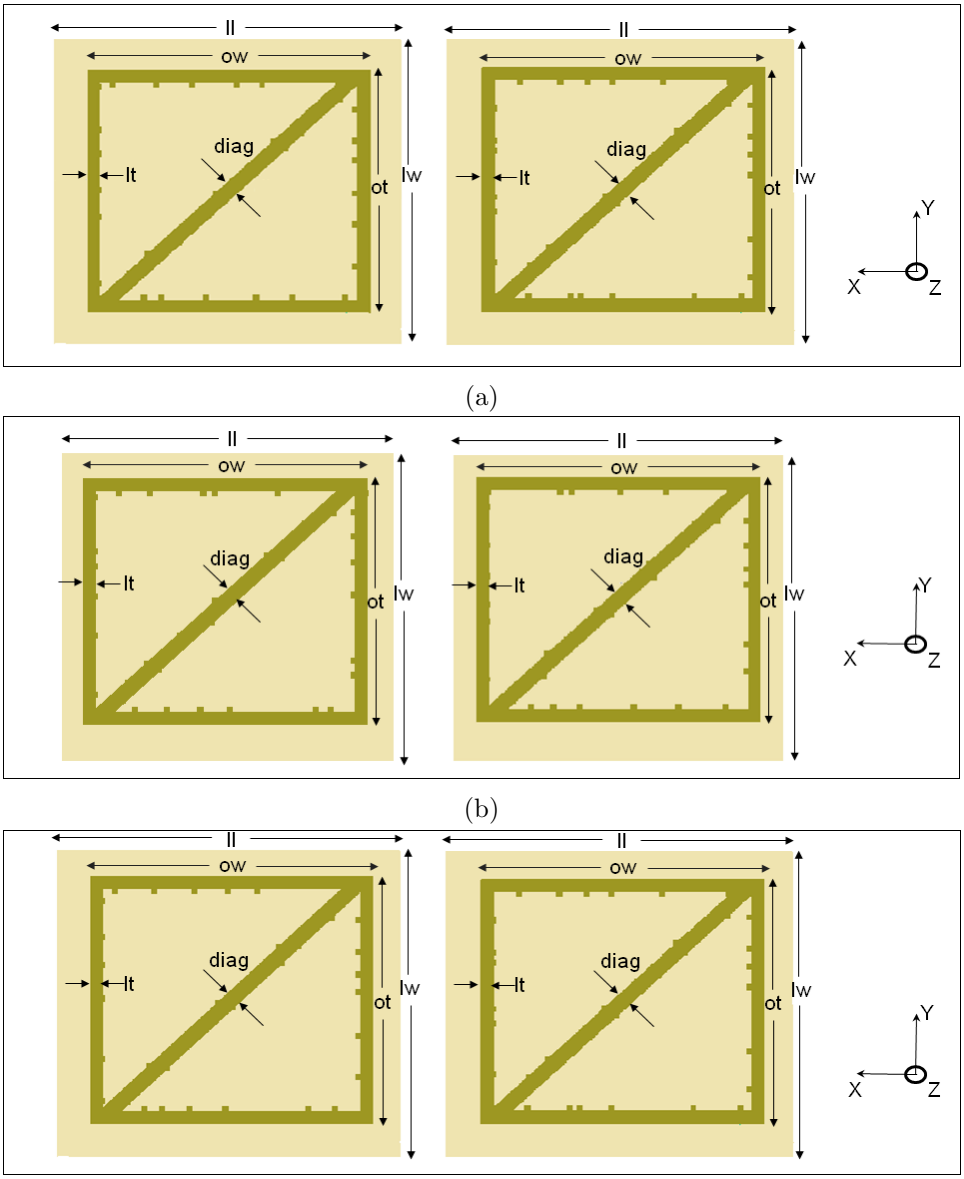

Figure 4.8: Unit cells containing roughness along the inner periphery of the rectangular loop and the diagonal causing (a) maximum and minimum return loss bandwidths respectively, (b) maximum and minimum gains respectively and (c) maximum and minimum axial ratios respectively.

metasurface containing roughness in the inner periphery of the rectangular loop and the diagonal in the unit cell.

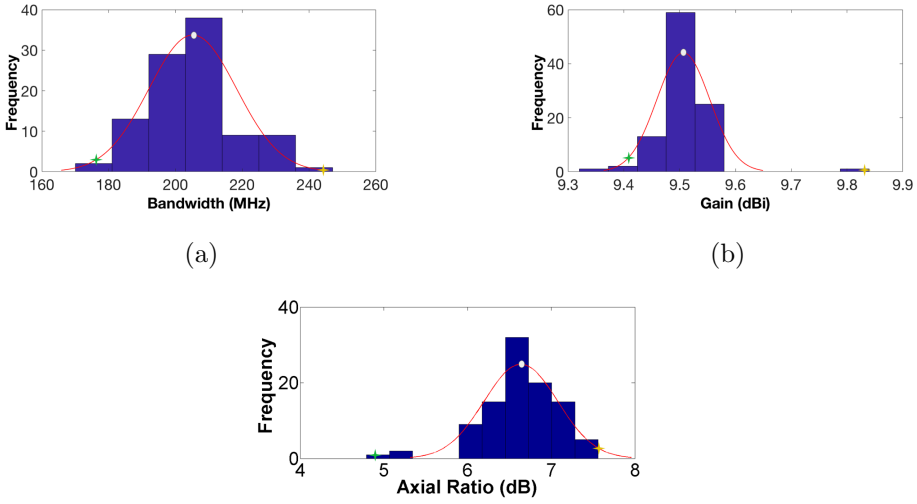

(a) (b)

(c)

Figure 4.9: Histogram depicting variations for hundred different designs of metasurface superstrate with roughness present inside the periphery of the rectangular loop and along the diagonal for (a) return loss bandwidth, (b) gain and (c) axial ratio. The peak of red curve denotes the mean bandwidth of the FPC antenna for all such hundred different designs.

We observe that maximum and minimum bandwidths out of all the hundred designs were 242.16 MHz (10.58%) and 177.76 MHz (7.76%), respectively. The mean bandwidth of all the hundred models was 205.17 MHz (8.96%). The maximum, minimum, and the mean gains are 9.84 dBi, 9.41 dBi, and 9.51 dBi, respectively. The maximum, minimum, and the mean axial ratio were 7.47 dB, 4.79 dB and 6.66 dB respectively.

4.5 Analysis of FPC antenna with metasurface with roughness present on both sides of periphery of rectangular loop and diagonal

In the next step, we introduced roughness both inside and outside the periphery of the rectangular loop and the diagonal by adding bricks in them. MATLAB software was used to generate hundred positions of these bricks along the periphery of the rectangular loop and the diagonal through randomization of the brick position. Fig. 4.10 (a)-(c) denote the roughened metasurface designs on both sides of the peripheries of the rectangular loop

and the diagonal for maximum and minimum bandwidths, gains and axial ratios respectively.

Simulations were performed for these hundred different designs to obtain return loss bandwidth, gain, and axial ratio. Histogram was performed to obtain distributions for the bandwidth, gain, and axial ratio for these designs. We observe that the bandwidth is drastically reduced on introducing roughness on the outer periphery of the rectangular loop. We also observed a slight degradation in the gain and reduction in the axial ratio of the FPC antenna. Fig. 4.11 (a)-(c) denote the histogram for the bandwidth, gain and the axial ratio for the roughened metasurface with roughness present on both the peripheries of the rectangular loop and the diagonal.

From the histogram, we can see that the maximum, minimum, and the mean bandwidth of hundred FPC antenna with different roughened metasurface designs is 113.26 MHz (4.91%), 58.824 MHz (2.56%) and 90.143 MHz (3.92%) respectively. The maximum, minimum and the mean gain was 9.43 dBi , 8.97 dBi and 9.21 dBi, whereas the maximum, minimum and the mean axial ratio was around 5.4 dB ,4.03 dB and 4.79 dB respectively. The mean gain slightly declined by 0.3 dBi, and the mean axial ratio decreased by around 1.87 dB.

Therefore we can see that FPC antenna with metasurface with roughness present in the inner periphery of the rectangular loop and the diagonal in the unit cell has better return loss bandwidth, gain, and reduced axial ratio as compared to that with smooth rectangular loop and the diagonal in the unit cell. However, when roughness was added in the outer rectangular loop periphery, there was a drastic reduction in return loss bandwidth, but further improvement in the axial ratio. We conclude that both these designs convert linearly polarised signal from the simple patch antenna into a circularly polarized signal.

The metasurface design with roughness present in the inner periphery of the rectangular loop and the diagonal causing minimum axial ratio shown in Fig. 4.8 (c) caused the return loss bandwidth of 202.78 MHz (8.86%), gain of 9.48 dBi and axial ratio of 4.79 dB. This was the best metasurface design which produced optimum bandwidth, gain and axial ratio.

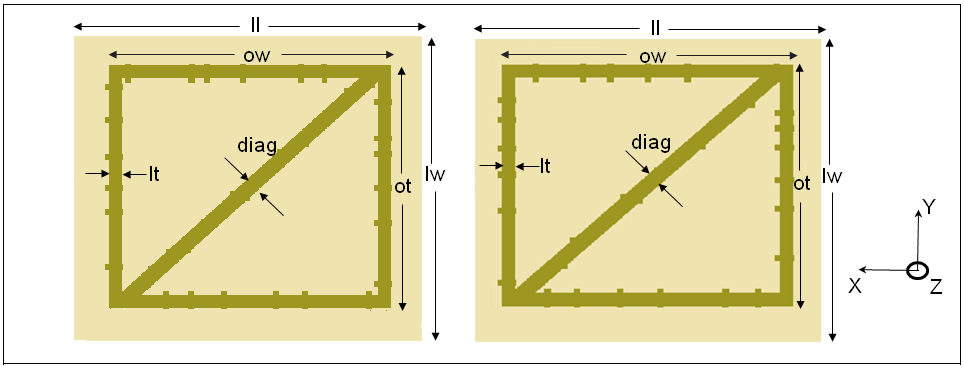

(a)

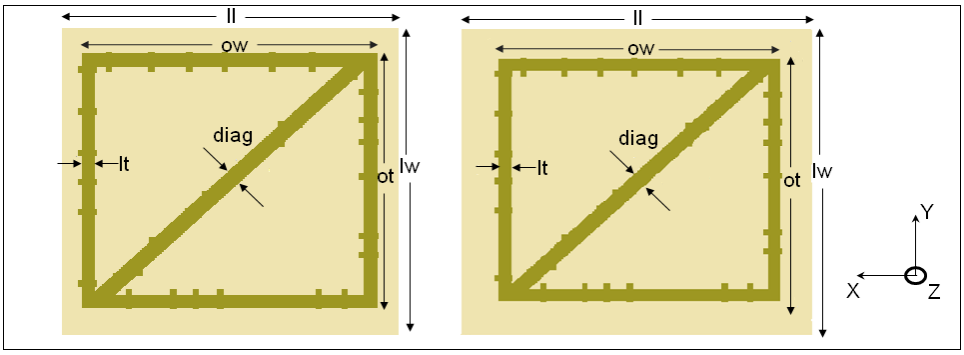

(b)

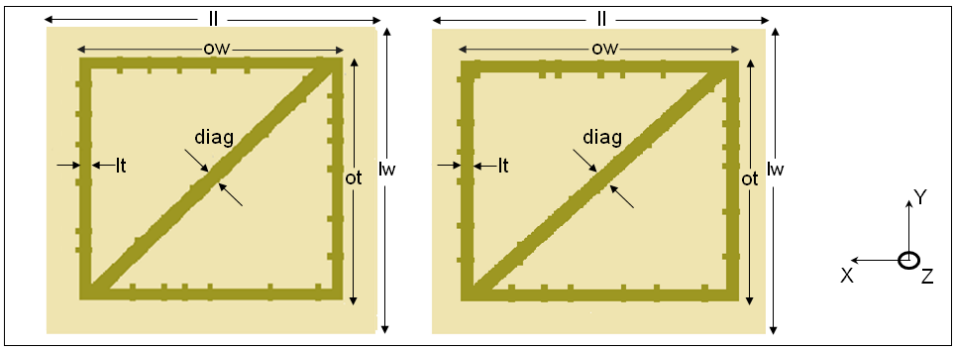

(c)

Figure 4.10: Unit cells containing roughness on both the peripheries of the rectangular loop and the diagonal causing (a) maximum and minimum return loss bandwidths respectively, (b) maximum and minimum gains respectively and (c) maximum and minimum axial ratios respectively.

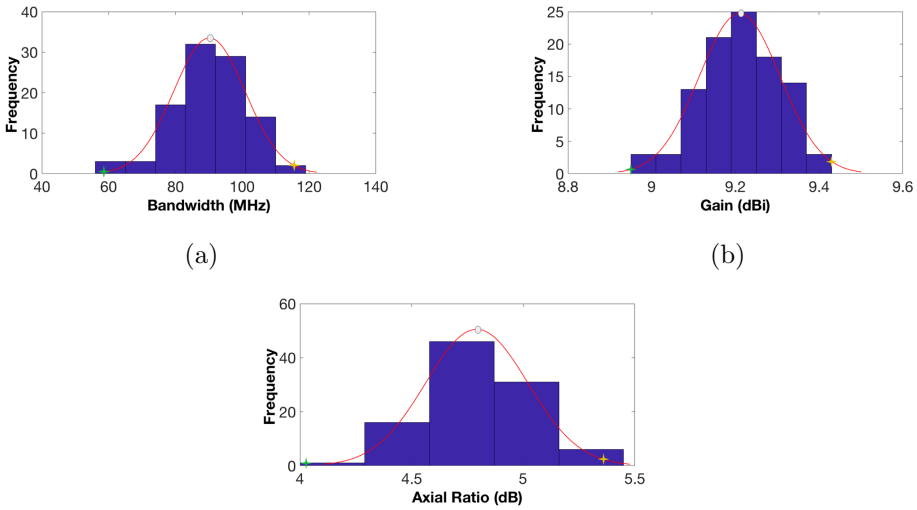

(a) (b)

(c)

Figure 4.11: Histogram depicting variations for hundred different designs of metasurface superstrate layer with roughness present on both sides of the periphery of the rectangular loop and the diagonal in the unit cell for (a) return loss bandwidth (b) gain and (c) axial ratio. The peak of the red curve denotes the mean of the all hundred different designs of FPC antenna.

Chapter 5

Conclusion

In this thesis, we introduced two new designs of FPC antennas. The first design consisted of a metasurface with a unit cell with an arc with roughness around its periphery. The second consisted of a metasurface with a unit cell with a rectangular loop with a diagonal with roughness along its periphery. The objective of both designs was to obtain a circular polarized antenna without compromising bandwidth and gain.

We observed that introducing the metasurface superstrate layer with both the arc and rectangular loop with diagonal in the unit cell enhanced the gain and bandwidth and significantly decreased the axial ratio. However, the latter was more effective in doing so than the former. Roughness along the arc periphery improved the gain and reduced the axial ratio. However, there was a decline in bandwidth. Roughness in the inner periphery as opposed to both the inner and outer periphery of the rectangular loop and the diagonal of the metasurface further decreased the axial ratio and improved the gain and bandwidth. We achieved a minimum axial ratio 4.79 dB for a return loss bandwidth of 202.78 MHz (8.86%) and gain of 9.48 dBi.

Bibliography

[1] C. A. Balanis, *Antenna theory: analysis and design*. John wiley & sons, 2016.

[2] R. Orr, G. Goussetis, and V. Fusco, "Design method for circularly polarized fabry–perot cavity antennas," *IEEE Transactions on Antennas and Propagation*, vol. 62, no. 1, pp. 19–26, 2013.

[3] Z.-g. Liu, "Fabry-perot resonator antenna," *Journal of Infrared, Millimeter, and Terahertz Waves*, vol. 31, no. 4, pp. 391–403, 2010.

[4] ——, "Effect of primary source location on fabry-perot resonator antenna," in *2009 Asia Pacific Microwave Conference*. IEEE, 2009, pp. 1809–1812.

[5] H. Boutayeb and T. A. Denidni, "Internally excited fabry-perot type cavity: power normalization and directivity evaluation," *IEEE Antennas and Wireless Propagation Letters*, vol. 5, pp. 159–162, 2006.

[6] Z. Liu, "Quasi-periodic structure application in fabry-perot resonator printed antenna," in *2008 Asia-Pacific Microwave Conference*. IEEE, 2008, pp. 1–4.

[7] J. Winn, J. Joannopoulos, S. Johnson, and R. D. Meade, "Photonic crystals: Molding the flow of light," *Princeton University Press, Princeton, NJ*, vol. 6, pp. 2059–2062, 1995.

[8] D. Sievenpiper, L. Zhang, R. F. Broas, N. G. Alexopolous, E. Yablonovitch *et al.*, "High-impedance electromagnetic surfaces with a forbidden frequency band," *IEEE Transactions on Microwave Theory and techniques*, vol. 47, no. 11, pp. 2059–2074, 1999.

[9] A. R. Weily, K. P. Esselle, B. C. Sanders, and T. S. Bird, "High-gain 1d ebg resonator antenna," *Microwave and Optical Technology Letters*, vol. 47, no. 2, pp. 107–114, 2005.

[10] M. Thévenot, J. Drouet, R. Chantalat *et al.*, "Improvements for the ebg resonator antenna," *EurCap*, 2006.

[11] H. Yang and N. Alexopoulos, "Gain enhancement methods for printed circuit antennas through multiple superstrates," *IEEE Transactions on Antennas and Propagation*, vol. 35, no. 7, pp. 860–863, 1987.

[12] G. V. Trentini, "Partially reflecting sheet arrays," *IRE Transactions on Antennas and Propagation*, vol. 4, no. 4, pp. 666–671, 1956.

[13] D. Jackson and N. Alexopoulos, "Gain enhancement methods for printed circuit antennas," *IEEE transactions on antennas and propagation*, vol. 33, no. 9, pp. 976–987, 1985.

[14] D. R. Jackson and A. A. Oliner, "A leaky-wave analysis of the high-gain printed antenna configuration," *IEEE Transactions on Antennas and Propagation*, vol. 36, no. 7, pp. 905–910, 1988.

[15] Z. Liu, W. Zhang, D. Fu, Y. Gu, and Z. Ge, "Broadband fabry-perot resonator printed antennas using fss superstrate with dissimilar size," *Microwave and Optical Technology Letters*, vol. 50, no. 6, pp. 1623–1627, 2008.

[16] Y. Hao, A. Alomainy, and C. Parini, "Antenna-beam shaping from offset defects in uc-ebg cavities," *Microwave and Optical Technology Letters*, vol. 43, no. 2, pp. 108–112, 2004.

[17] A. Ourir, S. Burokur, and A. De Lustrac, "Phase-varying metamaterial for compact steerable directive antennas," *Electronics letters*, vol. 43, no. 9, pp. 493–494, 2007.

[18] D. Pozar, "An update on microstrip antenna theory and design including some novel feeding techniques," *IEEE Antennas and Propagation Society Newsletter*, vol. 28, no. 5, pp. 4–9, 1986.

[19] K. Carver and J. Mink, "Microstrip antenna technology," *IEEE transactions on antennas and propagation*, vol. 29, no. 1, pp. 2–24, 1981.

[20] Z.-G. Liu, Z.-X. Cao, and L.-N. Wu, "Compact low-profile circularly polarized fabry–perot resonator antenna fed by linearly polarized microstrip patch," *IEEE Antennas and Wireless Propagation Letters*, vol. 15, pp. 524–527, 2015.

[21] F. Costa, S. Genovesi, and A. Monorchio, "On the bandwidth of high-impedance frequency selective surfaces," *IEEE Antennas and Wireless Propagation Letters*, vol. 8, pp. 1341–1344, 2009.

[22] H. Zhu, S. Cheung, K. L. Chung, and T. I. Yuk, "Linear-to-circular polarization conversion using metasurface," *IEEE Transactions on Antennas and Propagation*, vol. 61, no. 9, pp. 4615–4623, 2013.

[23] A. K. Singh, M. P. Abegaonkar, and S. K. Koul, "High-gain and high-aperture-efficiency cavity resonator antenna using metamaterial superstrate," *IEEE Antennas and Wireless Propagation Letters*, vol. 16, pp. 2388–2391, 2017.